How to cite: *Angew. Chem. Int. Ed.* **2023**, *62*, e202313564
doi.org/10.1002/anie.202313564

*Solid-State Chemistry*

# Combining Nitridoborates, Nitrides and Hydrides—Synthesis and Characterization of the Multianionic $Sr_6N[BN_2]_2H_3$

*Sophia L. Wandelt, Alexander Mutschke, Dmitry Khalyavin, Robert Calaminus, Jennifer Steinadler, Bettina V. Lotsch, and Wolfgang Schnick**

**Abstract:** Multianionic metal hydrides, which exhibit a wide variety of physical properties and complex structures, have recently attracted growing interest. Here we present $Sr_6N[BN_2]_2H_3$, prepared in a solid-state ampoule reaction at 800 °C, as the first combination of nitridoborate, nitride and hydride anions within a single compound. The crystal structure was solved from single-crystal X-ray and neutron powder diffraction data in space group $P2_1/c$ (no. 14), revealing a three-dimensional network of undulated layers of nitridoborate units, strontium atoms and hydride together with nitride anions. Magic angle spinning (MAS) NMR and vibrational spectroscopy in combination with quantum chemical calculations further confirm the structure model. Electrochemical measurements suggest the existence of hydride ion conductivity, allowing the hydrides to migrate along the layers.

Metal hydrides gained significant interest in research over the last decades, acting as catalysts, luminescent materials or hydride ion conductors.[1–3] Next to their intriguing physical properties, metal hydrides are characterized by a large structural diversity that comprises manifold coordination environments and bonding partners of the hydrogen anion.[4] It can be surrounded by the respective metal cations in a linear, trigonal planar, tetrahedral, trigonal bipyramidal or even octahedral fashion.[5–8] In such materials, the respective metal hydride bond lengths vary from 1.6 to 3.0 Å. Introducing other metals or non-metals can even lead to complex anions such as $[BH_4]^-$ or $[NiH_4]^{4-}$.[9–10] Similarly, the nitride anion shows a wide variety of coordination environments. It is often found in complex $[NH_4]$, $[BN_x]$, $[PN_4]$ or $[SiN_4]$ moieties, but can also appear as an isolated $N^{3-}$ ion. Binary metal nitrides hereby comprise diverse structural environments, ranging from coordination number two (linear) up to nine (capped quadratic antiprism).[11–18] The metal nitride distances differ significantly from 1.4 to 2.8 Å. The incorporation of other anions into the respective compound provides a new platform of structures and functionalities. By combining different ionic radii, polarizabilities and electronegativities within one material, its properties can be tailored on demand.[19] While oxide hydrides and fluoride hydrides are the most prominent classes of multinary hydrides due to their high stability and easy accessibility, the field of nitride hydrides just established itself as functionally and structurally diverse. For instance, $Ba_5CrN_4H$ and $Ca_6[Cr_2N_6]H$ show catalytic activity and magnetism, while $Ca_2NH$ and $Sr_2LiH_2N$ convince with hydrogen storage capacity and ion conductivity, respectively.[20–23] At the same time, they form diverse structures comprising complex $[Cr_2N_6]^{11-}$ anions or double chains of edge-sharing $N(Sr_5Li)$ and $H(Sr_5Li)$ octahedra. Nitridoborate hydrides containing complex $[N–B–N]^{3-}$ ions are another emerging group of structurally intriguing salt-like metal hydrides.[24] Starting with $Ca_2BN_2H$ in 2004, this class combines highly stable nitridoborate ions next to the elusive hydride ions within one material.[25–26] When it comes to multinary compounds with three or more different anions, the hydride family is only sparsely explored yet, with $SmH_{0.78}OF_{0.22}$ and $Sr_2LiHOCl_2$ being just two recent members.[27–28] Due to the high reactivity and omnipresent abundance of oxygen, this class exclusively consists of hydride oxides. Neither an oxide-free nor a complex anion containing compound was found to date with such a multianionic composition.

In this contribution, we present the strontium nitridoborate nitride hydride $Sr_6N[BN_2]_2H_3$, which connects the two emerging fields of nitride hydrides and nitridoborate hydrides. Moreover, the oxide-free heteroanionic compound containing $H^-$, $N^{3-}$ and $[BN_2]^{3-}$ anions possibly exhibits two-dimensional hydride ion conductivity.

[*] S. L. Wandelt, R. Calaminus, J. Steinadler, Prof. Dr. B. V. Lotsch, Prof. Dr. W. Schnick
Department of Chemistry, University of Munich (LMU)
Butenandtstr. 5–13, 81377 Munich (Germany)
E-mail: wolfgang.schnick@uni-muenchen.de

Dr. A. Mutschke
Chair of Inorganic Chemistry with Focus in Novel Materials, Department of Chemistry, TU Munich
Lichtenbergstr. 4, 85748 Garching (Germany)
and
Heinz Maier-Leibnitz Zentrum (MLZ), TU Munich
Lichtenbergstr. 1, 85748 Garching (Germany)

Dr. D. Khalyavin
Rutherford Appleton Laboratory, ISIS Neutron and Muon Source
Didcot OX11 0QX (UK)

R. Calaminus, Prof. Dr. B. V. Lotsch
Max Planck Institute for Solid State Research
Heisenbergstr. 1, 70569 Stuttgart (Germany)

$Sr_6N[BN_2]_2H_3$ was obtained in a solid-state reaction of stoichiometric amounts of $Sr_2N$, $SrH_2$ and $Sr_3B_2N_4$ in a tantalum ampoule at 800 °C, yielding colorless block-like crystals. The crystal structure was partially solved based on single-crystal X-ray diffraction (XRD) data (Table 1), in which only the crystallographic positions of Sr, B and N could be determined reliably with X-ray data due to the low scattering power of hydrogen. Rietveld refinement based on powder XRD data of the bulk sample shows $SrH_2$ (5.5 (2) wt %) and $Sr_3B_2N_4$ (2.1(1) wt %) as minor side phases (Figure S1 in the Supporting Information). To reliably locate the hydrogen position in the structure, time-of-flight neutron powder diffraction data of the isotypic deuterated compound $Sr_6N[^{11}BN_2]_2D_3$ were collected. Additional isotope substitution with $^{11}B$ was necessary to avoid neutron absorption caused by $^{10}B$. Rietveld refinement based on neutron powder diffraction data (Table 1, Figure S2) corroborate the proposed structure model with deuterium on two crystallographically independent sites coordinated by strontium atoms. While D1 is located on a fully occupied position inside a tetrahedron, D2 shows a split position with 50 % occupancy within a distorted square planar coordination environment (Figure 1). Due to its comparatively large coordination sphere, the hydride anion shifts toward shorter Sr–H distances, resulting in two strongly distorted trigonal planar coordinated positions. The difference Fourier map calculated from the refined neutron diffraction data with unoccupied deuterium positions ($Sr_6N[^{11}BN_2]_2\square_3$) exhibits accordingly two distinct maxima of the core density at the D2 position (Figure 1). Crystallographic data of the X-ray and neutron refinements are listed in Tables S1 and S2.[29]

***Table 1:*** Crystallographic data of the single-crystal XRD refinement and Rietveld refinement based on neutron powder diffraction data of $Sr_6N[BN_2]_2H_3$ and $Sr_6N[^{11}BN_2]_2D_3$, respectively.

| formula | $Sr_6N[BN_2]_2H_3$ | $Sr_6N[^{11}BN_2]_2D_3$ |
|---|---|---|
| space group | $P2_1/c$ (no. 14) | |
| lattice parameters/Å, ° | $a=6.6778(8)$ | $a=6.6821(2)$ |
| | $b=11.387(1)$ | $b=11.3884(4)$ |
| | $c=7.7311(9)$ | $c=7.7416(2)$ |
| | $\beta=107.459(5)$ | $\beta=107.534(2)$ |
| cell volume/Å$^3$ | 560.8(1) | 561.75(3) |
| formula units/unit cell | 2 | |
| molecular weight/g·mol$^{-1}$ | 620.41 | 623.81 |
| temperature/K | 293(2) | 298(1) |
| diffractometer | Bruker D8 Venture | WISH @ ISIS |
| radiation | Mo-K$\alpha$ ($\lambda=0.71973$ Å) | neutrons, *time-of-flight* |
| refined parameters | 69 | 70 |
| goodness of fit | 1.077 | 8.240 |
| *R* indices | $R1[I\geq2\sigma(I)]=0.0220$ | $R_p=0.0411$ |
| | $wR2[I\geq2\sigma(I)]=0.0499$ | $R_{wp}=0.0591$ |
| | $R1$(all data) $=0.0262$ | $R_{exp}=0.0072$ |
| | $wR2$(all data) $=0.0509$ | $R_{Bragg}=0.0661$ |

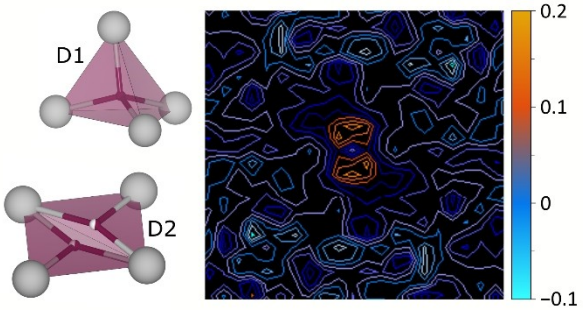


***Figure 1.*** Illustration of the deuteride coordination spheres in $Sr_6N[^{11}BN_2]_2D_3$ (left), where the hydride atoms and polyhedra are displayed in purple and the Sr atoms in gray. Fourier map calculated from neutron diffraction data at the crystallographic position of D2 (right), the orange lines indicate residual core density.

$Sr_6N[BN_2]_2H_3$ exhibits a three-dimensional network consisting of alternating undulated layers of $[BN_2]^{3-}$ units, Sr atoms and hydride together with nitride anions (Figure 2a). Two of the Sr ions show a distorted octahedral coordination by two hydride and four nitrogen anions (Figure 2b), whereas the third Sr is found inside a $Sr(N_5B_2H_3)$ polyhedron, as previously seen in $Sr_{13}[BN_2]_6H_8$.[24] The coordination sphere of the $[BN_2]^{3-}$ units can be described as a bicapped trigonal prism (Figure 2c) which is also found in β-$Ba_3[BN_2]_2$.[30] The $[BN_2]^{3-}$ unit itself is slightly bent with an N–B–N angle of 169.4(5)° and shows N–B bond lengths of 1.329(7)–1.353 (7) Å, which are in good agreement with other known nitridoborates.[31–32] The isolated $N^{3-}$ ions are octahedrally coordinated by Sr atoms (Figure 2c) with expected Sr–N bond lengths of 2.549(4)–2.685(4) Å.[32–33] As mentioned above, the hydride ions are coordinated tetrahedrally and in a distorted trigonal planar fashion by $Sr^{2+}$ (Figure 1). Both show Sr–H bond lengths of 2.47(1)–2.79(1) Å in accordance with literature data.[26,34–35]

Firstly, $Sr_6N[BN_2]_2H_3$ seems to be structurally related to the compounds $(Sr_6N)[MN_2][CN_2]_2$ (*M*=Co, Fe, Cu) and $M_2[CN_2]Cl_2$ (*M*=Sr, Eu), which feature the same layer-like structure and isoelectronic $[N–C–N]^{2-}$ units.[36–39] But taking a closer look at the network reveals that the coordination polyhedra and orientation of the $[CN_2]^{2-}$ units along the

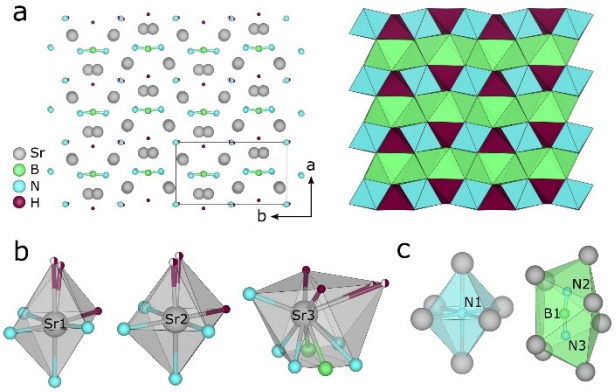


***Figure 2.*** Illustration of the crystal structure of $Sr_6N[BN_2]_2H_3$. (a) Alternating undulated layers of Sr atoms, $[BN_2]^{3-}$ units and hydride and nitride anions (left) and respective polyhedra (right), both viewed along [001]. (b) $Sr(N_4H_2)$ octahedra and $Sr(N_5B_2H_3)$ polyhedron, (c) octahedrally coordinated $N^{3-}$ anion and $[BN_2]^{3-}$ unit coordinated by strontium atoms in a bicapped trigonal prism. The Sr atoms and respective polyhedra are displayed in gray, N in blue, B in green and H in purple.

layers vary significantly from those of our $[BN_2]^{3-}$ units. However, the compounds $AE_3BX_2$ ($AE$=Ca or Sr, $B$=$[C_3]^{4-}$ or $[CBN]^{4-}$ and $X$=Cl or Br) show more structural similarities to our title compound $Sr_6N[BN_2]_2H_3$.[40–42] The isoelectronic allenylide and carbonitridoborate units show a similar arrangement and coordination polyhedra as our nitridoborate units. The $X1$ position is equally to the H1 position tetrahedrally coordinated by the respective alkaline earth metals, whereas $X2$ is inside a quadratic planar environment. However, as the strontium ions are shifted in $Sr_6N[BN_2]_2H_3$, the nitride and H2 ions are octahedrally and distorted trigonally planar coordinated, respectively.

Our proposed structure model is further validated by $^1$H and $^{11}$B MAS NMR measurements. The $^1$H spectrum (Figure 3, top) shows a main signal at 6.6 ppm originating from the two crystallographically independent $H^-$ positions within the structure. Since the local environments of both positions are very similar, the chemical shift values are expected to be almost identical. In addition, homonuclear dicouplings between the hydrides lead to a broadening of the resonance lines, so that the two contributions are not resolved in the MAS spectrum. However, the shift of the $^1$H resonance position towards positive $\delta_{iso}$ values is usually characteristic for protonic hydrogen and negative values are expected for hydrides. But as already observed in other metal hydrides and further discussed by Hosono et al., the metal-hydride distances have a significant influence on the chemical shift, resulting in the observed positive $\delta_{iso}$ for salt-like hydrides.[26,43–45] Minor impurities of $Sr_2NH$ and an unknown side phase cause the two additional signals at 7.0 and 1.2 ppm, respectively.

The shape of the central transition signal in the $^{11}$B MAS spectrum (Figure 3, bottom) is dominated by the interaction between the quadrupolar moment of $^{11}$B ($I$=3/2) and the electric field gradient (EFG) within the unit cell. Due to the asymmetric charge distribution around the B atoms in the $[BN_2]^{3-}$ units, the observed line shape exhibits a characteristic broadening and is consistent with a single crystallographic site. Using the DMFIT program, values for the quadrupolar coupling constant (3.28 MHz) and the asymmetry parameter (0.05) were obtained as well as an isotropic chemical shift of 24.3 ppm.[46] Considering a N–B–N bond angle of 169.4°, these results fit nicely into the series of NMR parameters reported so far for nearly linear $[BN_2]^{3-}$ units in other nitridoborates.[24,47]

As hydride and the complex nitridoborate anions can both be infrared and Raman active, vibrational spectroscopy is another suitable method to analyze our compound. The experimental FTIR spectrum of $Sr_6N[BN_2]_2H_3$ (Figure 4) agrees well with the simulated one, which was obtained by DFT calculations at the PBE0 level of theory. The strong bands of the N–B–N vibrations arise at 1652 cm$^{-1}$ (antisymmetrical stretching, $\nu_2$) and 599 cm$^{-1}$ (out-of-plane bending, $\nu_3$), which agrees well with the literature, as the $\nu_2$ and $\nu_3$ vibrations are usually expected at around 1700 and 600 cm$^{-1}$, respectively.[48] Hydride in-plane and out-of-plane vibrations, in which the hydride ion vibrates inside its strontium coordination sphere, can be observed at 919, 815 and 697 cm$^{-1}$, agreeing with literature.[24–25] The weak band at 1725 cm$^{-1}$ is caused by N–B–N vibrations of the side phase $Sr_3B_2N_4$. Furthermore, any OH or NH species can be excluded, as there are no vibrations visible in the region of 3600–3200 cm$^{-1}$ (Figure S3). The Raman spectrum is also in good agreement with the simulated one (Figure S4). At 1057 cm$^{-1}$ appears the strong N–B–N symmetrical stretching ($\nu_2$), which is also in good accordance with related

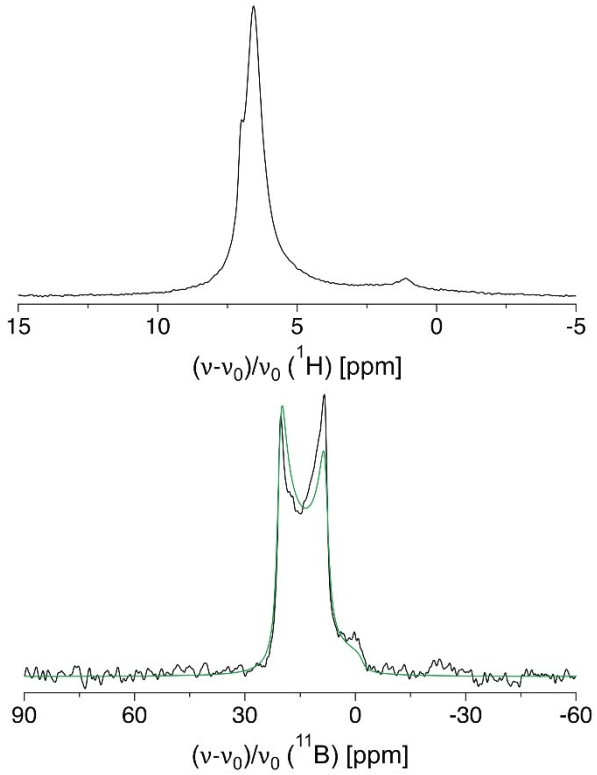


***Figure 3.*** $^1$H (top) and $^{11}$B (bottom) MAS NMR spectrum of $Sr_6N[BN_2]_2H_3$ at 20 kHz spinning frequency. The best fitting result of the $^{11}$B signal is shown as a green line.

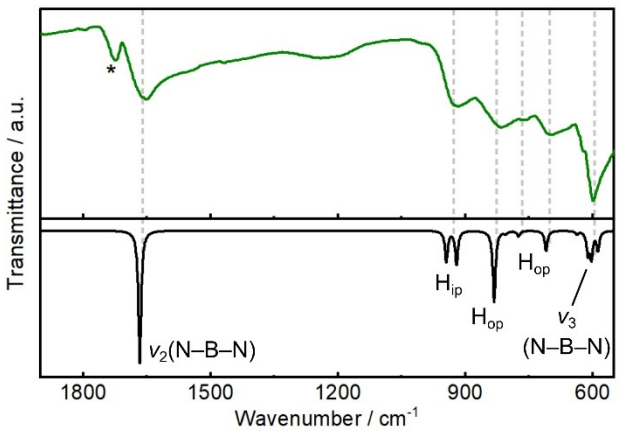


***Figure 4.*** Experimental (top) and simulated (obtained by DFT-PBE0 calculations, bottom) FTIR spectrum of $Sr_6N[BN_2]_2H_3$. The band marked with an asterisk arises from the side phase $Sr_3B_2N_4$.

compounds.[49] Between 600 and 623 $cm^{-1}$ the $H^-$ out-of-plane vibrations and the N–B–N out-of-plane bending ($\nu_3$) are detectable. Below 300 $cm^{-1}$, the bands of the isotropic lattice vibrations are visible. The plane of the different vibrations is described by the respective layers of nitridoborate and hydride ions. The assignment of IR and Raman vibrations can be found in Tables S3 and S4.

As the layer-like structure provides a suitable prerequisite for two-dimensional migration of the hydride ions, we performed electrochemical impedance spectroscopy (EIS) and chronopotentiometry to evaluate possible ionic conductivity. The EIS measurement (Figure S5) shows an imperfect semicircle without a polarization tail, indicating a mixed ionic and electronic conductor. Taking both conduction processes into account, a fit of the spectrum revealed an electronic conductivity of $6.3\times10^{-10}$ S/cm and an ionic conductivity of $3.3\times10^{-9}$ S/cm at 75 °C.[50] To further confirm the conductivity values, we performed chronopotentiometry measurements (Figure S7), which yielded a similar value for the electronic conductivity and a smaller value for the ionic conductivity. The difference is discussed in the SI. Taking a closer look on the thermal displacement ellipsoids from X-ray and neutron diffraction data, the ones of the hydride ions are rather large and elongated, whereas all other atoms are in a normal range. Therefore, we assume that hydride ions are the conducting species in our compound. Moreover, softBV calculations support this thesis, as they yield a low activation barrier for $H^-$ and rather large values for $Sr^{2+}$ (Figures S8 and S9).[51–53] Further details of the measurements and calculations can be found in the Supporting Information. Compared to other hydride ion conductors such as $Sr_2LiH_{2.2}O_{0.2}N_{0.8}$ ($7.2\times10^{-6}$ S/cm at 300 °C) or $La_2LiHO_3$ ($3.85\times10^{-6}$ S/cm at 275 °C), $Sr_6N[BN_2]_2H_3$ shows a lower conductivity, which may be attributed to the relatively low measurement temperature of 75 °C.[54–55] However, the ionic conductivity at 300 °C can be estimated using the Arrhenius equation, yielding an ionic conductivity of $5.8\times10^{-7}$ S/cm at 300 °C (Figure S10), which is in the range of other known hydride ion conductors.

The electronic structure of $Sr_6N[BN_2]_2H_3$ was investigated by quantum chemical calculations that were performed at the DFT-PBE0 level of theory. The crystal structure was optimized and determined to be a true local minimum without imaginary frequencies. The optimized lattice parameters $a$, $b$, $c$, and $\beta$ deviate by −0.6 %, −0.05 %, −0.6 % and 0.1 %, respectively, from the experimental data. The calculated electronic band structure (Figure S11, left) reveals a direct band gap of 4.1 eV, which agrees with the transparent and colorless appearance of $Sr_6N[BN_2]_2H_3$. Similarly to the two other nitridoborate hydrides $Sr_2BN_2H$ and $Sr_{13}[BN_2]_6H_8$, the projected density of states (Figure S11, right) shows nitrogen at the top of the valence band with small contributions of Sr.[24,26] Interestingly, since both N and Sr states contribute to the top of the valence band, covalent interactions of N with Sr are indicated. This is also suggested by bond overlap population analysis (see SI) which indeed reveal considerable overlap between the isolated $N^{3-}$ and $Sr^{2+}$.

Summing up, we have obtained the new strontium nitridoborate nitride hydride $Sr_6N[BN_2]_2H_3$ from a solid-state reaction at 800 °C. Combining single-crystal X-ray and neutron powder diffraction data, the crystal structure was elucidated. It reveals a novel three-dimensional network consisting of alternating undulated layers of strontium atoms, $[BN_2]^{3-}$ units and $N^{3-}$ together with $H^-$ ions. Further analyses such as MAS NMR, vibrational spectroscopy and quantum chemical calculations complement the structural analysis. Additionally, the new compound seems to exhibits ionic conductivity, enabling the hydride ions to migrate in a two-dimensional manner along the [011] plane.

## Supporting Information

The authors have cited additional references within the Supporting Information.[33,51–53,56–80]

## Acknowledgements

The authors gratefully acknowledge the ISIS Neutron and Muon Source for granting beamtime (proposal no. 2220086) and financial support by the DFG under Germany's Excellence Strategy—EXC 2089/1-390776260 (e-conversion). Robert Calaminus gratefully acknowledges the German Federal Ministry of Education and Research (BMBF) for their financial support through the FestBatt project 03XP0430B. The authors thank Christian Minke (Department of Chemistry, LMU Munich) for the MAS NMR measurements. Open Access funding enabled and organized by Projekt DEAL.

## Conflict of Interest

The authors declare no conflict of interest.

## Data Availability Statement

The data that support the findings of this study are available in the supplementary material of this article.

**Keywords:** Hydride Ion Conductor · Hydrides · Neutron Diffraction · Nitrides · Nitridoborates

[1] M. Kitano, J. Kujirai, K. Ogasawara, S. Matsuishi, T. Tada, H. Abe, Y. Niwa, H. Hosono, *J. Am. Chem. Soc.* **2019**, *141*, 20344.
[2] N. Kunkel, H. Kohlmann, *J. Phys. Chem. C* **2016**, *120*, 10506.
[3] Y. Yu, W. Zhang, H. Cao, T. He, P. Chen, *Trends Chem.* **2022**, *4*, 935.
[4] C. Janiak, H.-J. Meyer, D. Gudat, R. Alsfasser, E. Riedel, *Moderne anorganische Chemie*, De Gruyter, Berlin **2012**.
[5] R. Sato, H. Saitoh, N. Endo, S. Takagi, M. Matsuo, K. Aoki, S.-I. Orimo, *Appl. Phys. Lett.* **2013**, *102*, 091901.
[6] C. Weidenthaler, T. J. Frankcombe, M. Felderhoff, *Inorg. Chem.* **2006**, *45*, 3849.

[7] T. V. Blankenship, M. J. Dickman, L. J. v. d. Burgt, S. E. Latturner, *Inorg. Chem.* **2015**, *54*, 914.
[8] F. Altorfer, W. Bührer, B. Winkler, G. Coddens, R. Essmann, H. Jacobs, *Solid State Ionics* **1994**, *70*, 272.
[9] G. Renaudin, L. Guénée, K. Yvon, *J. Alloys Compd.* **2003**, *350*, 145.
[10] M. Matsuo, A. Remhof, P. Martelli, R. Caputo, M. Ernst, Y. Miura, T. Sato, H. Oguchi, H. Maekawa, H. Takamura, A. Borgschulte, A. Züttel, S.-I. Orimo, *J. Am. Chem. Soc.* **2009**, *131*, 16389.
[11] X. Zhao, K. J. Range, *J. Alloys Compd.* **2000**, *296*, 72.
[12] A. Brager, *Acta Physicochim. URSS* **1937**, *7*, 699.
[13] G. A. Jeffrey, G. S. Parry, R. L. Mozzi, *J. Chem. Phys.* **1956**, *25*, 1024.
[14] P. Eckerlin, A. Rabenau, *Z. Anorg. Allg. Chem.* **1960**, *304*, 218.
[15] D. Fischer, Z. Cancarevic, J. C. Schön, M. Jansen, *Z. Anorg. Allg. Chem.* **2004**, *630*, 156.
[16] J. Hao, Q. L. Cui, G. Zou, J. Liu, X. Li, Y. Li, Q. L. Zhou, D. Iiu, M. Li, F. Li, W. W. Lei, W. Chen, Y. Ma, *Inorg. Chem.* **2009**, *48*, 9737.
[17] E. Zintl, G. Brauer, *Z. Elektrochem. Angew. Phys. Chem.* **1935**, *41*, 102.
[18] G. V. M. Vajenine, X. Wang, I. Efthimiopoulos, S. Karmakar, K. Syassen, M. Hanfland, *Phys. Rev. B* **2009**, *79*, 224107.
[19] H. Kageyama, K. Hayashi, K. Maeda, J. P. Attfield, Z. Hiroi, J. M. Rondinelli, K. R. Poeppelmeier, *Nat. Commun.* **2018**, *9*, 772.
[20] Y. Guan, W. Zhang, Q. Wang, C. Weidenthaler, A. Wu, W. Gao, Q. Pei, H. Yan, J. Cui, H. Wu, S. Feng, R. Wang, H. Cao, X. Ju, L. Liu, T. He, J. Guo, P. Chen, *Chem Catal.* **2021**, *1*, 1042.
[21] M. S. Bailey, M. N. Obrovac, E. Baillet, T. K. Reynolds, D. B. Zax, F. J. DiSalvo, *Inorg. Chem.* **2003**, *42*, 5572.
[22] P. Chen, Z. Xiong, J. Luo, J. Lin, K. L. Tan, *Nature* **2002**, *420*, 302.
[23] G. Jiang, N. Matsui, T. Mezaki, Y. Toda, K. Suzuki, M. Hirayama, T. Saito, T. Kamiyama, R. Kanno, *J. Solid State Chem.* **2022**, *310*, 123051.
[24] S. L. Wandelt, A. Mutschke, D. Khalyavin, J. Steinadler, W. Schnick, *Chem. Eur. J.* **2023**, *29*, e202301241.
[25] M. Somer, Ö. Yaren, O. Reckeweg, Y. Prots, W. Carrillo-Cabrera, *Z. Anorg. Allg. Chem.* **2004**, *630*, 1068.
[26] S. L. Wandelt, A. Karnas, A. Mutschke, N. Kunkel, C. Ritter, W. Schnick, *Inorg. Chem.* **2022**, *61*, 12685.
[27] N. Zapp, H. E. Fischer, H. Kohlmann, *Inorg. Chem.* **2021**, *60*, 17775.
[28] Z. Wei, H. Ubukata, C. Zhong, C. Tassel, H. Kageyama, *Inorg. Chem.* **2023**, *62*, 7993.
[29] Deposition numbers 2279203 (for $Sr_6N[BN_2]_2H_3$) and 2279204 (for $Sr_6N[^{11}BN_2]_2D_3$) contain the supplementary crystallographic data for this paper. These data are provided free of charge by the joint Cambridge Crystallographic Data Centre and Fachinformationszentrum Karlsruhe Access Structures service.
[30] O. Reckeweg, F. J. DiSalvo, M. Somer, *J. Alloys Compd.* **2003**, *361*, 102.
[31] M. Häberlen, J. Glaser, H.-J. Meyer, *J. Solid State Chem.* **2005**, *178*, 1478.
[32] S. F. Matar, A. F. A. Alam, R. Pöttgen, *Z. Naturforsch. B* **2017**, *72*, 433.
[33] O. Reckeweg, F. J. DiSalvo, *Solid State Sci.* **2002**, *4*, 575.
[34] B. Blaschkowski, T. Schleid, *Z. Anorg. Allg. Chem.* **2007**, *633*, 2644.
[35] F. Rohrer, R. Nesper, *J. Solid State Chem.* **1998**, *135*, 194.
[36] J. K. Bendyna, P. Höhn, W. Schnelle, R. Kniep, *Sci. Technol. Adv. Mater.* **2007**, *8*, 393.
[37] J. K. Bendyna, P. Höhn, R. Kniep, *Z. Kristallogr.* **2009**, *224*, 5.
[38] W. P. Clark, R. Niewa, *Z. Anorg. Allg. Chem.* **2020**, *646*, 114.
[39] W. Liao, R. Dronskowski, *Z. Anorg. Allg. Chem.* **2005**, *631*, 496.
[40] H. Womelsdorf, H.-J. Meyer, *Z. Anorg. Allg. Chem.* **1994**, *620*, 258.
[41] H.-J. Meyer, *Z. Anorg. Allg. Chem.* **1991**, *593*, 185.
[42] H.-J. Meyer, *Z. Anorg. Allg. Chem.* **1991**, *594*, 113.
[43] A. Mutschke, G. M. Bernard, M. Bertmer, A. J. Karttunen, C. Ritter, V. K. Michaelis, N. Kunkel, *Angew. Chem. Int. Ed.* **2021**, *60*, 5683.
[44] K. Hayashi, P. V. Sushko, Y. Hashimoto, A. L. Shluger, H. Hosono, *Nat. Commun.* **2014**, *5*, 3515.
[45] A. Mutschke, A. Schulz, M. Bertmer, C. Ritter, A. J. Karttunen, G. Kieslich, N. Kunkel, *Chem. Sci.* **2022**, *13*, 7773.
[46] D. Massiot, F. Fayon, M. Capron, I. King, S. L. Calvé, B. Alonso, J. O. Durand, B. Bujoli, Z. Gan, G. Hoatson, *Magn. Reson. Chem.* **2002**, *40*, 70.
[47] S. Seidel, T. Dierkes, T. Jüstel, C. Benndorf, H. Eckert, R. Pöttgen, *Dalton Trans.* **2016**, *45*, 12078.
[48] R. Pöttgen, O. Reckeweg, *Z. Kristallogr.* **2017**, *232*, 653.
[49] I. Kokal, U. Aydemir, Y. Prots, W. Schnelle, L. Akselrud, P. Höhn, M. Somer, *Z. Kristallogr.* **2011**, *226*, 633.
[50] R. A. Huggins, *Ionics* **2002**, *8*, 300.
[51] H. Chen, L. L. Wong, S. Adams, *Acta Crystallogr. Sect. B* **2019**, *75*, 18.
[52] H. Chen, S. Adams, *IUCrJ* **2017**, *4*, 614.
[53] L. L. Wong, K. C. Phuah, R. Dai, H. Chen, W. S. Chew, S. Adams, *Chem. Mater.* **2021**, *33*, 625.
[54] A. J. E. Rowberg, L. Weston, C. G. V. d. Walle, *J. Phys. Chem. C* **2021**, *125*, 2250.
[55] Y. Iwasaki, N. Matsui, K. Suzuki, Y. Hinuma, M. Yonemura, G. Kobayashi, M. Hirayama, I. Tanaka, R. Kanno, *J. Mater. Chem. A* **2018**, *6*, 23457.
[56] A. F. Holleman, N. Wiberg, *Lehrbuch der Anorganischen Chemie*, De Gruyter, Berlin **2007**.
[57] T. Wylezich, R. Valois, M. Suta, A. Mutschke, C. Ritter, A. Meijerink, A. J. Karttunen, N. Kunkel, *Chem. Eur. J.* **2020**, *26*, 11742.
[58] G. M. Sheldrick, SADABS Version 2: Multi-Scan Absorption Correction, Bruker-AXS, Madison, Wisconsin, USA **2012**.
[59] Bruker-AXS, XPREP Reciprocal Space Exploration, Vers. 6.12, Karlsruhe, Germany **2001**.
[60] Bruker-AXS, APEX3, Vers. 2016.5-0, Karlsruhe, Germany **2016**.
[61] G. M. Sheldrick, *Acta Crystallogr. Sect. A* **2008**, *64*, 112.
[62] G. M. Sheldrick, SHELXS - A Program for Crystal Structure Solution, University of Göttingen, Göttingen, Germany **1997**.
[63] A. Coelho, TOPAS-Academic V6.1, Coelho Software, Brisbane, Australia **2007**.
[64] H. M. Rietveld, *J. Appl. Crystallogr.* **1969**, *2*, 65.
[65] L. C. Chapon, P. Manuel, P. G. Radaelli, C. Benson, L. Perrott, S. Ansell, N. J. Rhodes, D. Raspino, D. Duxbury, E. Spill, J. Norris, *Neutron News* **2011**, *22*, 22.
[66] J. Rodriguez-Carvajal, *Physica B + C* **1993**, *192*, 55.
[67] V. F. Sears, *Neutron News* **1992**, *3*, 26.
[68] A. D. McNaught, A. Wilkinson, *IUPAC. Compendium of Chemical Terminology*, Blackwell Scientific Publications, Oxford **1997**.
[69] J. P. Perdew, K. Burke, M. Ernzerhof, *Phys. Rev. Lett.* **1996**, *77*, 3865.
[70] C. Adamo, V. Barone, *J. Chem. Phys.* **1999**, *110*, 6158.
[71] R. Dovesi, A. Erba, R. Orlando, C. M. Zicovich-Wilson, B. Civalleri, L. Maschio, M. Rérat, S. Casassa, J. Baima, S. Salustro, B. Kirtman, *Wiley Interdiscip. Rev.: Comput. Mol. Sci.* **2018**, *8*, e1360.
[72] F. Weigend, R. Ahlrichs, *Phys. Chem. Chem. Phys.* **2005**, *7*, 3297.

[73] A. J. Karttunen, T. Tynell, M. Karppinen, *J. Phys. Chem. C* **2015**, *119*, 13105.
[74] H. J. Monkhorst, J. D. Pack, *Phys. Rev. B* **1976**, *13*, 5188.
[75] A. Togo, I. Tanaka, arXiv:1808.01590 [cond-mat.mtrl-sci] **2018**.
[76] Y. Hinuma, G. Pizzi, Y. Kumagai, F. Oba, I. Tanaka, *Comput. Mater. Sci.* **2017**, *128*, 140.
[77] F. Pascale, C. M. Zicovich-Wilson, F. L. Gejo, B. Civalleri, R. Orlando, R. Dovesi, *J. Comput. Chem.* **2004**, *25*, 888.
[78] C. M. Zicovich-Wilson, F. Pascale, C. Roetti, V. R. Saunders, R. Orlando, R. Dovesi, *J. Comput. Chem.* **2004**, *25*, 1873.
[79] L. Maschio, B. Kirtman, M. Rérat, R. Orlando, R. Dovesi, *J. Chem. Phys.* **2013**, *139*, 164101.
[80] J. T. S. Irvine, D. C. Sinclair, A. R. West, *Adv. Mater.* **1990**, *2*, 132.

Manuscript received: September 12, 2023
Accepted manuscript online: October 31, 2023
Version of record online: November 10, 2023